ULTRASTRUCTURE AND BIREFRINGENCE OF THE ISOLATED MITOTIC APPARATUS OF MARINE EGGS

LIONEL I. REBHUN and GRETA SANDER

From the Department of Biology, Princeton University, Princeton, New Jersey 08540 and the Marine Biological Laboratories, Woods Hole, Massachusetts 02543

ABSTRACT

Isolated mitotic apparatuses (MA) of clam and sea urchin eggs were investigated by polarizing and electron microscopy. Examination of fixed MA in oils of different refractive index revealed that at least 90% of the retardation of isolated MA is due to positive, form birefringence, the remaining retardation deriving from positive, intrinsic birefringence. Electron micrographs reveal the isolated MA to be composed of microtubules, ribosome-like particles, and a variety of vesicles. In the clam MA the number of vesicles and ribosome-like particles relative to the number of microtubules is much lower than in the sea urchin MA. In clam MA this allows form and intrinsic birefringence to be related directly to microtubules. The relation of birefringence to microtubules in isolated sea urchin MA is more complex since ribosome-like particles adhere to microtubules, are oriented by them, and are likely to contribute to the form birefringence of the isolated MA. However, comparison of values of retardation for clam and sea urchin MA, indicates that the major part of the birefringence in sea urchin MA is also due to microtubules. The interpretation of the structures giving rise to birefringence in the MA of the living cells is likely to be even more complex since masking substances, compression, or tension on the living MA may alter the magnitude or sign of the birefringence.

INTRODUCTION

The birefringence of the mitotic apparatus (MA) was first noted in fixed, pollen, mother cells of *Fritillaria* by Runnström (45) and in living *Rhynchelmis* eggs by Giklhorn (mentioned by Schmidt, reference 48). Runnström noted that in fixed plant cells and in marine eggs the birefringence was positive relative to the axis of the MA. All further work on MA from living cells (Schmidt, references 49 and 50, Swann, references 55 and 56; and Inoué, reference 15) has shown the sign of birefringence of the MA in the living cell to be positive relative to the long axis although asters in late anaphase may show a negative sign of birefringence (16). A number of observations on the birefringence of MA were made between 1928 and 1936 and are reviewed by Schmidt (50).

The first detailed use of birefringence in the interpretation of mitotic events on the molecular level appears to be that of Schmidt (51). The positive birefringence of asters and spindles was considered to arise from oriented protein chains. The changes in birefringence during anaphase were thought to arise from a contractile process in the chains which gives rise to chromosome movement. Birefringence and its changes were thus used to support the traction fiber hypothesis (28). In the work of Swann (55, 56) on mitosis in sea urchin eggs, birefringence data were used to infer

molecular orientation or order–disorder changes in anaphase. In 1952, Inoué reported on the effects of colchicine (13) and temperature (14) on the birefringence of MA from eggs of the annelid *Chaetopterus*. He interpreted the data in terms of monomer–polymer transformations of a large unit and suggested that such transformations generated the motive force for chromosome movement (Inoué, reference 15).

In these cases, contraction of a protein fiber, order–disorder phenomena or polymerization–depolymerization changes were inferred from observations of birefringence in living cells. Unfortunately, little is really known concerning the molecules involved in birefringence or the manner in which changes in the properties of these molecules may be reflected in changes in the visible birefringence, although data, partly from electron microscope observations (Kane and Forer, reference 25) and partly from work on the chemistry of the isolated mitotic apparatus (Kane reference, 24, Stephens, reference 54, Sakai, reference 47), are now being gathered which may soon alter this situation.

Isolated MA were first shown to be birefringent by Mazia and Dan in 1952 (29). The first full paper on this property of the isolated MA, however, was not published until 1965 (25), when a correlation was established between the simultaneous disappearance of birefringence and microtubules; that paper implicated the microtubules as the ultrastructural species giving rise to birefringence. The initial intent of the present study was to investigate directly the correlation between microtubules and birefringence by relating the number and distribution of microtubules on the ultrastructural level with birefringence seen on the light microscope level. To this end, MA were isolated, fixed, and embedded in flat sheets of epoxy resin preparatory to sectioning selected areas in the MA. When the embedded material was examined with the polarizing microscope, it was found that all but a small amount of birefringence had disappeared. On further investigation, it was found that both sea urchin and surf clam MA possessed large, positive, form birefringence with a small, residual, positive, intrinsic birefringence. This result is in agreement with prior work by Pfeiffer (31). The virtual disappearance of MA birefringence in the embedded material was due to

TABLE I

Retardation of Background Material in Unfixed Strongylocentrotus purpuratus MA Isolated with Hexylene Glycol or Ethyl Cellosolve

Dates are those on which experiments were performed. Standard error given in parenthesis after average.

Hexylene glycol MA's			Ethyl cellosolve MA
29 May 1964		1 June 1964	4 March 1965
mμ		mμ	mμ
2.96		2.96	2.72
2.46	5.10 highest extinctions of	2.71	3.14
3.22	4.25 fibers in the MA	2.88	3.32
2.33		2.54	2.80
2.96		3.22	2.29
2.20		2.28	2.50
		2.54	2.47
			3.36
			2.33
			3.14
Avg 2.69 (0.17)		Avg 2.73 (0.12)	Avg 2.82 (0.13)

Standard deviations calculated from formula: $\text{SD} = \left(\frac{\Sigma\ (\text{Sample average})^2}{N-1}\right)^{1/2}$.

Standard error: from $\frac{\text{SD}}{N^{1/2}}$ where N is sample size.

TABLE II

Retardation of background and strongest fibers of S. purpuratus MA

MA were isolated in hexylene glycol and fixed in osmium tetroxide as described in the text. Standard error is given in parenthesis after the average.

Background	Fibers	Ratio of retardation of fibers/background
mμ	mμ	
2.96	4.24	1.43
2.28	3.56	1.56
2.28		
1.90		
1.69	2.20	1.30
1.69	2.12	1.25
1.90	2.46	1.29
1.90	2.54	1.34
1.10	2.12	1.93
1.87	2.64	1.41
2.54	3.40	1.34
1.10	2.04	1.85
2.04	2.96	1.45
2.20	3.47	1.58
1.72	2.71	1.58
Avg 1.94 (0.13)	Avg 2.80 (0.19)	Avg 1.49 (0.06)

the approximate match of refractive index of the epoxy resin to that of the MA, with the consequent elimination of most of the form birefringence.

This paper contains a general description of the MA of eggs of a clam, *Spisula solidissima*, and of a sea urchin, *Strongylocentrotus purpuratus*, as seen with the polarizing and electron microscopes and gives some quantitative data on their form and intrinsic birefringence. In addition, a correlation is established between the image of the MA in the electron microscope and that in the light microscope. In the case of *isolated* MA from *Spisula* eggs, this allows the implication to be drawn that it is the microtubules alone in the *isolated* MA which contribute the birefringence. This result directly contradicts a report recently published by Behnke and Forer (4), who claim that MA birefringence is *not* due to microtubules. Their work was done on in situ crane-fly spermatocyte MA whereas ours was done on *isolated* egg MA. Possible explanations of this difference in results will be offered.

A considerable number of the observations on birefringence in the MA of cells are reviewed by Hughes (12), Mazia (28), Inoué (15), and Swann (55, 56).

MATERIALS AND METHODS

Eggs from the purple sea urchin *Strongylocentrotus purpuratus* and the surf clam *Spisula solidissima* were used in this study. The urchins were obtained from Pacific Biomarine Supply Co., Venice, Calif. Urchins and clams were maintained in a large, closed, recirculating sea-water system and were used as needed. Mature eggs were fertilized or activated, and the mitotic apparatus was isolated at the appropriate time as described below. Three isolating media containing different organic reagents were used based on the results of Kane (22, 23): 12% solutions of hexylene glycol, of ethanol, or of ethoxyethanol (ethylcellosolve) in 0.02 M phosphate buffer at pH 6.1–6.2.

Fertilization membranes were removed from *S. purpuratus* eggs with thioethylgluconamide (30); the rest of the technique used to isolate MA was essentially the same as that described by Kane (20), except as noted below. Sea-urchin eggs were allowed to develop at about 18°–20°C. *S. solidissima* eggs were handled as previously described (37), except that isolation media were maintained at pH 6.2 rather than pH 6.5, and the eggs were parthenogenetically activated with KCl instead of being fertilized. The temperature of development used for *S. solidissima* eggs was 20°–23°C. Eggs of *S. purpuratus* or *S. solidissima*, at the appropriate stage of MA development

(first cleavage for *S. purpuratus*; first polar-body spindle stage for *S. solidissima*), were suspended in isolating medium for about 45 sec at room temperature, after which they were broken with a Vortex mixer. The homogenate was then poured into a 500 ml flask buried in ice; the flask then was swirled for cooling as rapidly as possible. The MA were collected and washed several times with isolating medium by low-speed centrifugation in the cold (4°C).

MA were observed either fixed or unfixed, as described in the tables and figure legends.

MA to be fixed were suspended in 1% OsO_4 or in 2.5% glutaraldehyde in isolating medium within 2 hr of initial isolation. Glutaraldehyde-fixed MA to be used for electron microscopy were postfixed in 1% OsO_4 in isolating medium. Fixed MA not used for immediate observation were dehydrated through a graded series of alcohols and transferred to propylene oxide. Some were then embedded in Epon 812 (27) for electron microscopy; the remainder were run into oils of various refractive indices (R. P. Cargille Laboratories, Inc., Cedar Grove, N. J.) for examination with phase and polarizing microscopes. In some cases, unfixed, isolated MA were rapidly frozen and then substituted by techniques described in detail elsewhere (34, 35). For this purpose, the MA were first suspended in 30% glycerol in the cold and then rapidly frozen. After freeze-substitution they were embedded in Epon 812 (27). Sections of all embedded MA were obtained with a Huxley (Cambridge Instrument Co., Inc., N. Y.) microtome or a Servall MT-2 microtome. The sections were stained with uranyl acetate (53) followed by lead citrate (39) and were examined in a Hitachi HU-11 electron microscope.

The phase microscope used was a Zeiss Winkel microscope. The polarizing microscope was a bench-type Inoué microscope with American-optical strain-free lenses (1). It was equipped with a 22.4 mμ retardation mica compensator and with 43 × strain-free lenses as objective and condenser.

The refractive index of fixed MA was measured by immersion refractometry (3, 40), i.e., by matching the MA with oils of different refractive indices. This would have been prohibitively difficult if the MA had not been fixed, since unfixed MA are almost invisible near the match point in the absence of the tan color imparted to MA by fixation in osmium tetroxide (see Observations). To be sure that a refractive index match had been reached MA were also examined in oils whose refractive indices were high enough to reverse the contrast of the MA from dark contrast (normal) to bright contrast, i.e., the refractive indices were greater than that of the MA. This can be seen by closely watching the halos at the edge of the MA since the halos are dark below the match point and bright above it. This method of matching is not very sensitive near the match point but can be used to estimate the refractive index of the MA to about 0.004. This is within the variability from MA to MA in a given batch.

Retardation was measured by the extinction method (1, 24). The compensator was rotated until the part of the MA observed was the darkest possible, and readings of the compensator angle were made at

TABLE III

Retardations of S. purpuratus MA

MA were isolated in ethanol and fixed in osmium tetroxide as described in Observations. Standard error is given in parentheses after the average.

Background	Fibers	Ratio of retardation of fibers/background
mμ	mμ	
3.98	5.08	1.28
3.82	5.08	1.33
4.15		
3.82	5.93	1.55
3.48		
4.32	5.93	1.37
3.14	4.15	1.32
3.48	4.92	1.41
2.80	4.40	1.57
2.80		
2.54		
3.05		
Avg 3.45 (0.17)	Avg 5.07 (0.26)	Avg 1.40 (0.05)

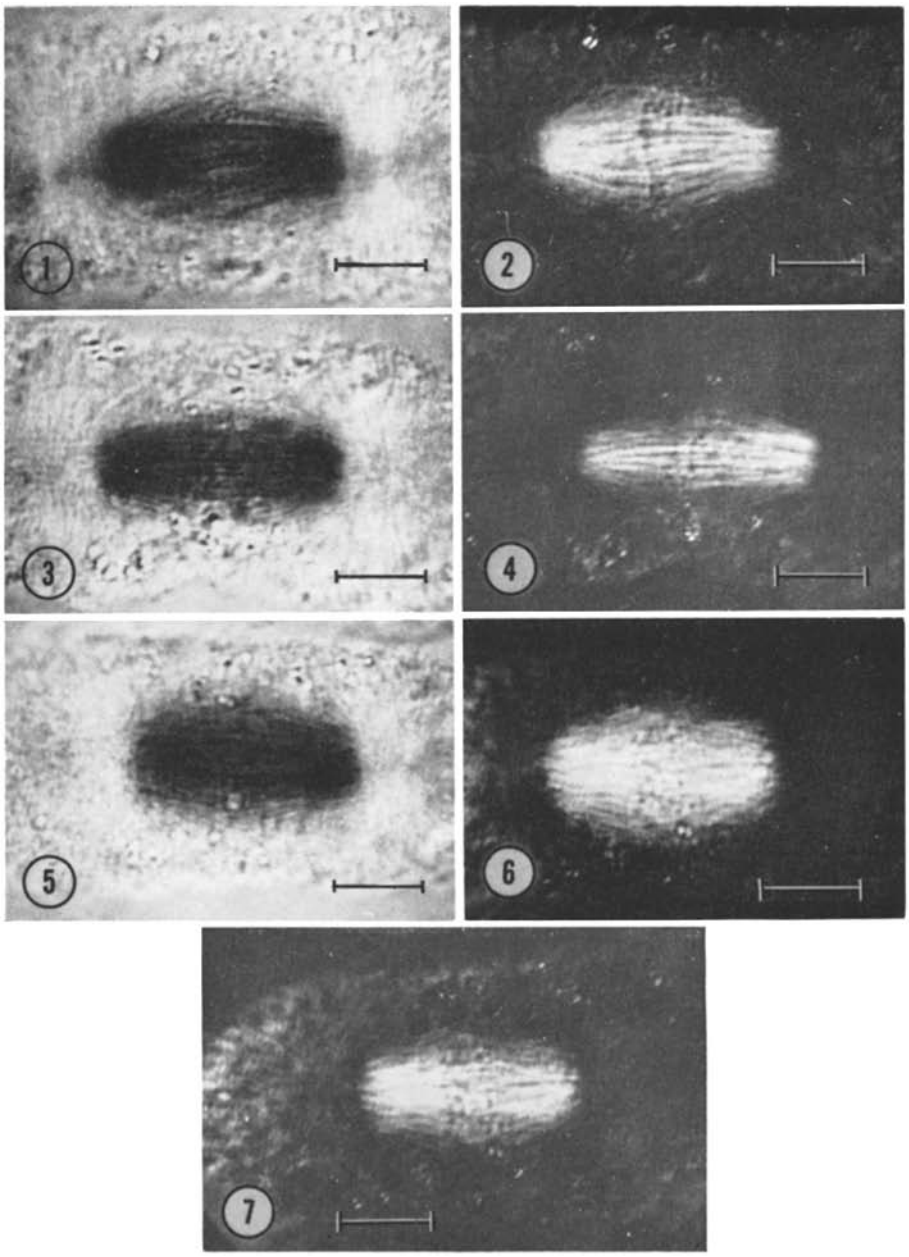

FIGURES 1 and 2 An unfixed, first cleavage MA of *S. purpuratus* at metaphase isolated in hexylene glycol. Fig. 1 is taken at $-4.0°$ and Fig. 2 at $+1.0°$ compensator settings. Note the strongly birefringent spindle fibers, weak astral birefringence and the considerable quantity of nonbirefringent material. Scale, 10 μ.

FIGURES 3 and 4 An *S. purpuratus* MA isolated as that in Figs. 1 and 2. Note the prominent spindle fibers. The MA is longer and narrower than that in Figs. 1 and 2. Fig. 3 is at $-3.0°$ and Fig. 4 at $+1.0°$ compensator settings. Scale, 10 μ.

FIGURES 5–7 An unfixed, *S. purpuratus* MA at the same stage and isolated as those in Figs. 1–4. Fig. 5 is at $-5.0°$, Fig. 6 at $0°$, and Fig. 7 at $-2.0°$ compensator settings. Fibers can be seen considerably better in Fig. 7 where background birefringence is partly compensated. Scale, 10 μ.

this point. Generally, the MA was measured in two quadrants at right angles to each other, the MA axis being at 45° to the polarizer axis in each quadrant, and the values were averaged. In most cases, the region immediately adjacent to and poleward of the chromosomes was measured. In *S. solidissima*, astral rays were also measured.

Retardation was obtained from the relation $\Gamma = -\Gamma_c \sin 2\theta$ where Γ is object retardation, Γ_c is maximum compensator retardation, and θ is extinction angle in radians (1, 26). Γ_c in our case is 22.4 mμ.

Photographs were taken with Plus X or Tri X film and were developed in Diafine developer (Baumann Photo-Chemical Corp).

OBSERVATIONS

Morphology of the Metaphase MA (Light Microscope Observations)

In all cases, MA at metaphase were used in the work described below. Metaphase MA of *S. solidissima* as seen with the phase microscope were described in a previous report (37). As background to the observations to be reported here, we shall summarize some of the results. Briefly, the MA consists of fibrous spindle and aster regions together with a small number of dark refractile bodies (about 1 μ) and a large number of clear vesicles the diameter of which may be as great as 3 μ. Chromosomes are present in the MA when first isolated and after one or two washings by centrifugation. After several cycles of washing, the MA tend to break up into isolated asters, spindles, or MA with only one aster. The meiotic chromosomes in general tend to be lost during washing. Adherent bits of cytoplasm can be seen on the MA after one or two washings, but these generally disappear after the third or fourth wash, the MA appearing quite "empty" except for fibers and vesicles. The astral rays are especially prominent

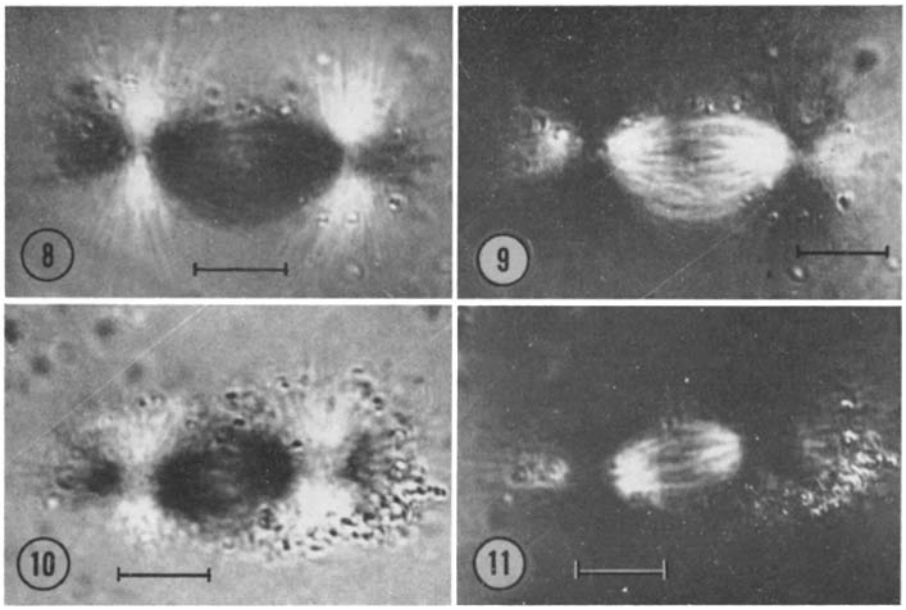

FIGURES 8 and 9 An unfixed, first polar body MA of *S. solidissima* isolated in hexylene glycol. Fig. 8 is at −3.0° and Fig. 9 at +1.0° compensator settings. Fibers both in the MA body and in asters are prominent and clear. The amount of nonbirefringent material is almost nonexistent, and the asters are strongly birefringent (as strong as the spindle proper). Scale, 10 μ.

FIGURES 10 and 11 Unfixed *S. solidissima* MA isolated as that in Figs. 8–9. Note that one aster is smaller than the other and the center-to-center distance is smaller than that in Figs. 8 and 9 by about 2 μ. Also, the central area of the spindle body has reduced birefringence except for continuous fibers. This may be a mid anaphase MA. Chromosomes have fallen off during preparation. Fig. 10 is at −5.0° compensator setting (retardation between pole and chromosome attachment point is 3.6 mμ). Fig. 11 is at a compensator setting of +1.0°. Scale, 10 μ.

and appear to protrude into the medium apparently devoid of any surrounding or embedding material. In contrast, examination of the MA of *S. purpuratus* with the phase microscope reveals that the fibrous material is surrounded by and embedded in nonfibrous material (20). In addition *S. purpuratus* MA are much more refractory to breakup during washing by centrifugation and are considerably less prone to lose their chromosomes

Considerable variations occur in the length and width of MA isolated at a given time from the same batch of eggs. This is especially true in MA of *S. purpuratus*, and is due to several factors: slight differences in intrinsic cleavage times in different eggs; differences in sperm-penetration times, which result in a spread of fertilization times; variations induced by the packing of eggs during centrifugation which unavoidably occurs at various times in the isolation procedure. An asynchrony, causing 3–4 min spreads in cleavage time (quite normal), will show considerable variability in exact stage of MA isolated. In *S. solidissima* eggs, which, in this study, are activated rather than fertilized and which have a longer metaphase than *S. purpuratus* eggs at the stage studied, these factors are less serious although some variability still occurs due primarily to variation in the time at which the MA migrates from the center of the egg where it is formed to the periphery where the polar bodies emerge (32). This migration is accompanied by a flattening of the peripheral aster so that the MA becomes asymmetric, and possesses one large spherical aster (central aster) and a more disc-shaped aster (peripheral aster) (6, 28, 32); e.g., compare Figs. 8 and 12.

The major morphological features of MA structure, as seen with the polarizing microscope, are essentially the same before and after fixation (see below). In most cases one can distinguish in the MA both a diffuse background birefringence and fibers in which the retardation is considerably

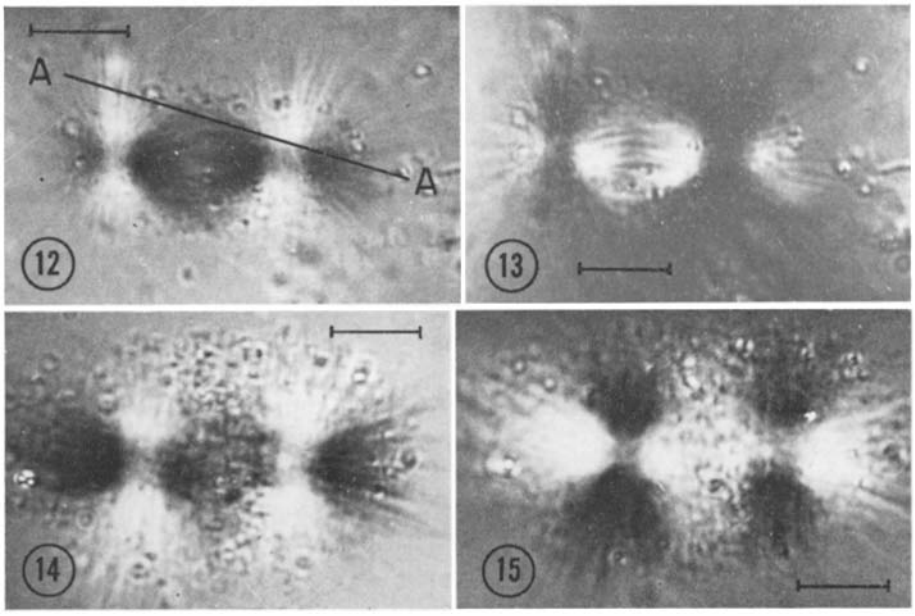

FIGURES 12 and 13 An unfixed *S. solidissima* MA isolated from the same batch of eggs as that in Figs. 10–11, at metaphase or very early anaphase. Fig. 12 is at −3.0° and Fig. 13 at +2.0° compensator settings. For significance of line A—A see legend for Fig. 24. Scale, 10 μ.

FIGURES 14 and 15 An unfixed *S. solidissima* MA isolated from a different batch of eggs from that used for MA in Figs. 12 and 13, but at about same stage and by the same technique. This preparation had more contamination, larger asters and smaller spindle body than usual. Compare with Figs. 8 and 9. Fig. 14 is at −3.0° and Figs. 15 at +2.0° compensator settings. Scale, 10 μ.

stronger than the background. This can be readily shown since the extinction point of the background occurs at compensator settings which are lower than those of the fibers. At the fiber-extinction setting of the compensator, the background is past its point of maximum darkening; the fibers thus appear dark on a lighter background (1) (Figs. 5–7). The fibers, corresponding to chromosomal fibers (52), are 0.5–1μ in diameter, the thicker ones having higher retardations. MA from *S. solidissima* generally show considerably more prominent fibers and considerably less background birefringence than those from *S. purpuratus*. Figs. 1–4 and 8–15 demonstrate the strong fibers in hexylene glycol–isolated MA of *S. purpuratus* and *S. solidissima* eggs, respectively.

For sea urchin MA, values for background retardation vary from 2.0–3.5 mμ in a given experiment. Fiber retardations are generally 20–50% higher than this, although in individual cases this range may be exceeded. Table I lists retardation values for the background of unfixed MA isolated in hexylene glycol and ethoxyethanol (Fig. 16), while Table II gives values for *S. purpuratus* MA isolated in hexylene glycol and fixed as described above. Retardations are listed for both background and fibers. The background retardation of fixed MA is lower than that of unfixed MA by about 28%.

Ethanol-isolated MA generally have higher retardations than MA isolated by the other reagents, with respect to both the background and the fibers; this applies especially to sea urchin MA. This can be seen from Table III which gives retardation values for fixed ethanol-isolated sea urchin MA. Figs. 17 and 18 show an unfixed ethanol-isolated MA of *S. purpuratus* in negative and positive contrast, while Figs. 19 and 20 show an osmium-tetroxide–fixed, ethanol-isolated MA of the same species.

In general the retardation of asters in the sea urchin at metaphase is considerably less than that of the spindle (Figs. 1–7, 16–20).

Observations on clam (*S. solidissima*) MA give results which are similar with respect to preservation of birefringence after fixation, presence of background and fiber birefringences, etc. However, in clam MA the predominant birefringence is that of the fibers, the background birefringence being considerably lower (Figs. 8–15). Also, the asters are strongly birefringent and, in some cases, their retardation exceeds that of the spindle, e.g., Figs. 8, 9, 12, 13. Retardations for three experiments are given in Table IV, the first two columns of which indicate values for unfixed spindle, and the last column of which indicates fixed spindles. A decrease in retardation of about 28% is seen after fixation of *S. solidissima* MA, this value being the same as that occurring after fixation of *S. purpuratus* MA. Retardations in this table are given for the strongest fibers in the MA and, as shown, retardations occasionally show great deviations from the average. The sign of the birefringence is positive with respect to the spindle axis for both clam and sea urchin MA. Figs. 21 and 22 are osmium-tetroxide–fixed, hexylene-glycol–isolated MA of *S.*

TABLE IV

Retardations of Fibers of Hexylene-Glycol—Isolated MA

MA were from first polar body stage of *S. solidissima*. Standard error is given in parenthesis after average.

30 May 1964 unfixed	2 June 1964 unfixed	4 June 1964 fixed as described in text
mμ	mμ	mμ
2.96	2.88	3.38
3.38	2.88	3.56
3.82	3.22	2.96
3.38	3.38	2.54
6.35*	4.66	1.86
	7.20*	2.96
Avg. 3.98 (0.61)	Avg. 4.04 (0.69)	Avg. 2.88 (0.25)

Average of 1st two columns, starred values omitted: 3.40

* Retardations rechecked several times.

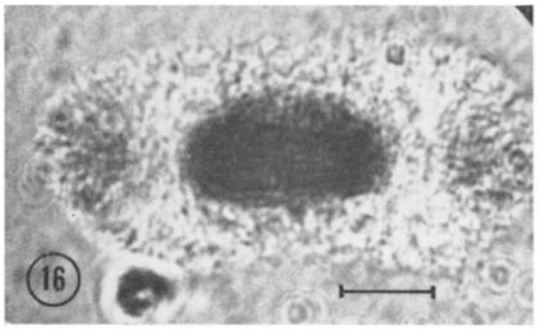

FIGURE 16 An unfixed MA isolated from first cleavage *S. purpuratus* eggs by the use of ethoxyethanol. The retardation midway between poles and spindle center is 3.5 mμ. Compensator setting for this micrograph was −5.0°. Scale, 10 μ.

TABLE V

Unfixed MA Isolated from S. purpuratus Eggs

Eggs were stored at 2°C for 16 days. Standard error is given in parentheses after average.

Retardation
mμ
0.84
1.52
0.89
0.84
0.72
0.89
0.89
0.18
0.84
1.10
Avg 0.97 (0.12)

solidissima and should be compared to unfixed MA in Figs. 8 and 9.

Stability of the Birefringence

Kane and Forer (25) have shown that MA left at room temperature decrease in retardation significantly in several hours. Decrease in retardation in MA stored in the cold is slower but also occurs. In our work we have also noted this decrease in retardation in stored, unfixed MA of both clam and sea urchin, although we find that the decrease in retardation is significantly less than that found by Kane and Forer (25), and that the decrease is less in clam than in sea urchin MA. Table V gives values for sea urchin MA isolated in hexylene glycol and stored unfixed at 0°C for 16 days. The values should be compared to those in Tables I–III. Clam MA isolated in hexylene glycol and stored for the same length of time show a similar decrease in retardation. Ethanol-isolated MA also show a proportionate decrease in retardation but become so highly light-scattering that measurements are exceedingly difficult to make.

Thus, a definite decrease in retardation occurs on storage of isolated MA although in our case the decrease is not so drastic as that reported by Kane and Forer (25). Nevertheless, because of this decrease, and for reasons mentioned below, fixed MA, whose birefringence is stable for months if stored at 0°–4°C in their isolating media, were used in most of this work.

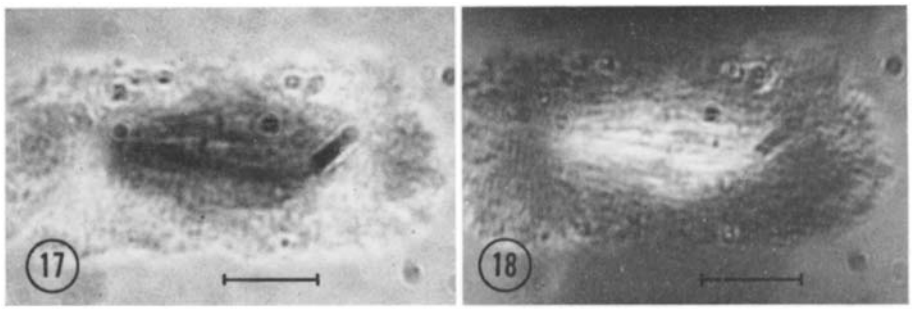

FIGURES 17 and 18 An unfixed MA isolated from first cleavage *S. purpuratus* egg by the ethanol technique. Note the strong, dense continuous fiber of retardation 3.1 mμ. This is unusually thick. In general, ethanol-isolated MA are greater in retardation and scatter light more than MA isolated by hexylene glycol. Fig. 17 is at −5.0° and Fig. 18 at +2.0° compensator settings. Scale, 10 μ.

Reaction with Fixatives

In general, isolated MA, when fixed with osmium tetroxide, turn different shades of brown or black depending on the medium in which they were isolated: ethanol-isolated MA turn black; MA isolated in hexylene glycol turn brown; and those isolated in ethoxyethanol turn a very light tan when the reaction is observed in the test tube. MA isolated in ethoxyethanol are generally fragile even after fixation, and they often, but not always, lose their birefringence as if unfixed. Because of this variability, only hexylene-glycol– and ethanol–isolated MA were used for further work in this study. In many cases an increase in light scattering, shown especially by adhering particles, accompanies fixation (Figs. 21 and 22).

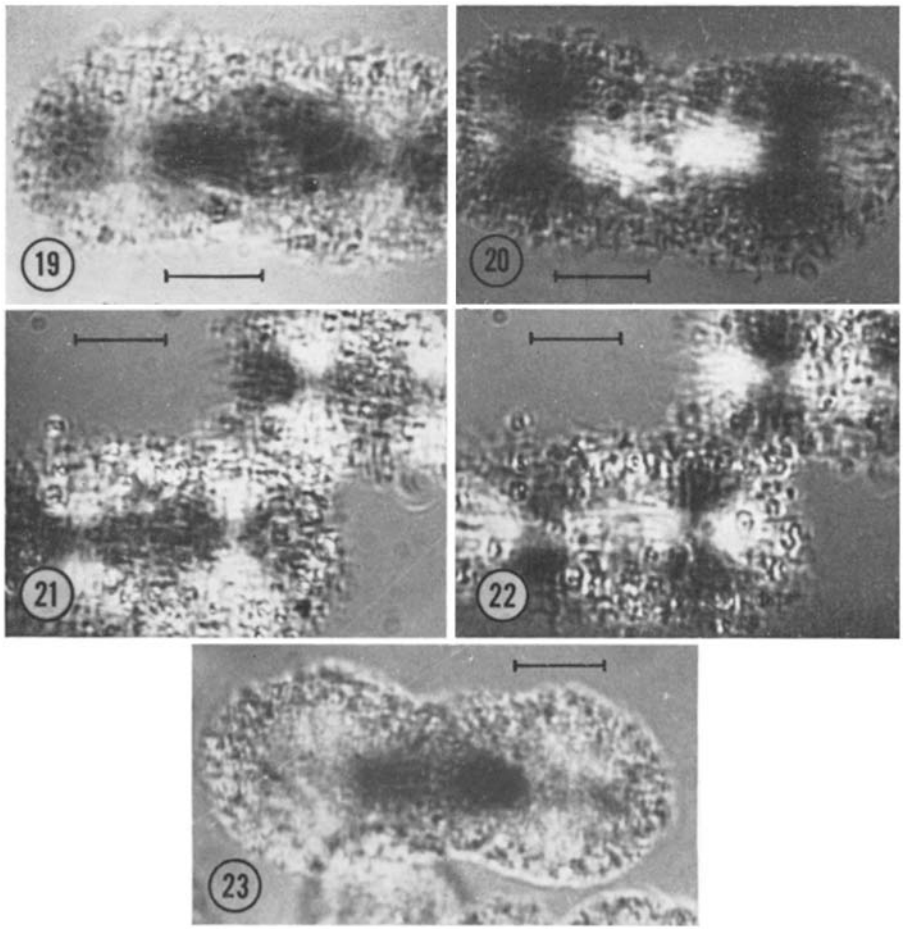

FIGURES 19 and 20 An ethanol-isolated, OsO_4-fixed first cleavage MA of *S. purpuratus* in 50% ethanol. Features of fixed, ethanol-dehydrated MA are very similar to those of unfixed MA if isolation is achieved with ethanol or hexylene glycol. Fig. 19 is at −3.0° and Fig. 20 at +2.0° compensator settings. Scale, 10 μ.

FIGURES 21 and 22 Hexylene-glycol–isolated, OsO_4-fixed first polar body MAs of *S. solidissima*. Retardation was lower than usual in this batch of eggs. Astral birefringence is 1.90 mμ. Note also greater contamination than in MA in Figs. 8–13. Scale, 10 μ.

FIGURE 23 Glutaraldehyde-fixed, hexylene-glycol–isolated MA of first cleavage *S. purpuratus* egg in absolute alcohol. Compare to Figs. 19 and 20 of OsO_4-fixed, ethanol-isolated MA. Compensator setting is −3.0°. Scale, 10 μ.

MA were also fixed in glutaraldehyde dissolved in the isolating medium. The birefringence was again preserved (Fig. 23). Unfortunately, glutaraldehyde-fixed MA clump into large masses when gathered by gentle centrifugation, a necessary procedure when transferring MA into various refractive-index oils. Since these masses can only be broken up by procedures which damage the MA, they proved unsuitable for measurement with the polarizing microscope because of excessive light-scattering of the clumps.

Refractive Index Measurements

Observations were made with a dark-contrast phase microscope equipped with a 43 × objective lens. As described in the Methods section, the halo at the edge of the MA was examined, and a match point was obtained when the halo disappeared (3, 40). For hexylene-glycol–isolated *S. solidissima* MA fixed in osmium tetroxide the refractive index (n) value is 1.588. For ethanol-isolated MA it is 1.620. In both cases, MA examined at n values 0.004 lower than these values have very faint but definite bright halos, and MA examined at n values 0.004 higher (1.592 for hexylene glycol and 1.624 for ethanol) the halos are dark, i.e., the phase of the MA relative to the surrounding oil is reversed. At the match point, however, variability is seen since some MA have slightly bright and some slightly dark halos; this is indicative of a slight variation in R.I. for different MA.

The corresponding match point value for *S. purpuratus* MA is 1.580 for hexylene-glycol–isolated MA and 1.60 for ethanol–isolated MA. The lower value for sea urchin MA is somewhat surprising since, in general, *unfixed* clam MA appear considerably more delicate and empty than unfixed sea urchin MA. However, the results are consistent and repeatable.

The MA appear homogeneous near the match point, i.e., no fibers can be seen inside them. In *S. solidissima* MA at the match point the astral fibers are recognizable with the phase microscope only by the tan color imparted by osmium-tetroxide fixation.

Retardation at the Match Point

In most cases a very slight retardation positive with respect to the spindle axis remains at the match point. The only exceptions to the observations of birefringence at the match point occur in some batches of ethanol–isolated MA which become unusually dark after osmium-tetroxide fixation. The heavy absorption of light makes observation inside the MA difficult and residual birefringence, if present, would be impossible to see.

TABLE VI

Estimated Retardations at the Match Point for fixed First polar body MA from Spisula

Standard error given in parentheses after average.

Hexylene-glycol–isolated MA*	Ethanol-isolated MA‡
$m\mu$	$m\mu$
0.30	0.51
0.13	0.67
0.38	0.67
0.47	0.84
0.21	
0.55	
Avg 0.34 (0.06)	Avg 0.67 (0.07)

* n = 1.588.

‡ n = 1.62; heavy absorption is due to reduced osmium tetroxide.

Accurate measurements of retardation at the match point are exceedingly difficult to make because the retardation is below 1 mμ (25). Table VI gives some retardation values obtained with *S. solidissima* MA. Although these values are undoubtedly in error by not less than 30%, they indicate the level of the retardation due to intrinsic birefringence. It was not possible to tell whether this retardation is due to background or to fibers. Similar relations hold for *S. purpuratus* MA although no exact measurements were attempted. It was determined, however, that the residual birefringence is <1 mμ.

Negatively Birefringent Fibers

On several occasions metaphase MA were seen which possessed a fiber showing an extinction at the opposite sign of compensator setting with respect to the rest of the spindle. That is, these fibers were dark when the MA was bright and vice versa. Each of these MA possessed one such negatively birefringent fiber whose retardation was in the neighborhood of 3–4 mμ (see reference 16 for discussion of possible causes for negative birefringence of astral fibers).

Electron Microscope Studies

Fig. 24 is an electron micrograph of an *S. solidissima* MA isolated in hexylene glycol and

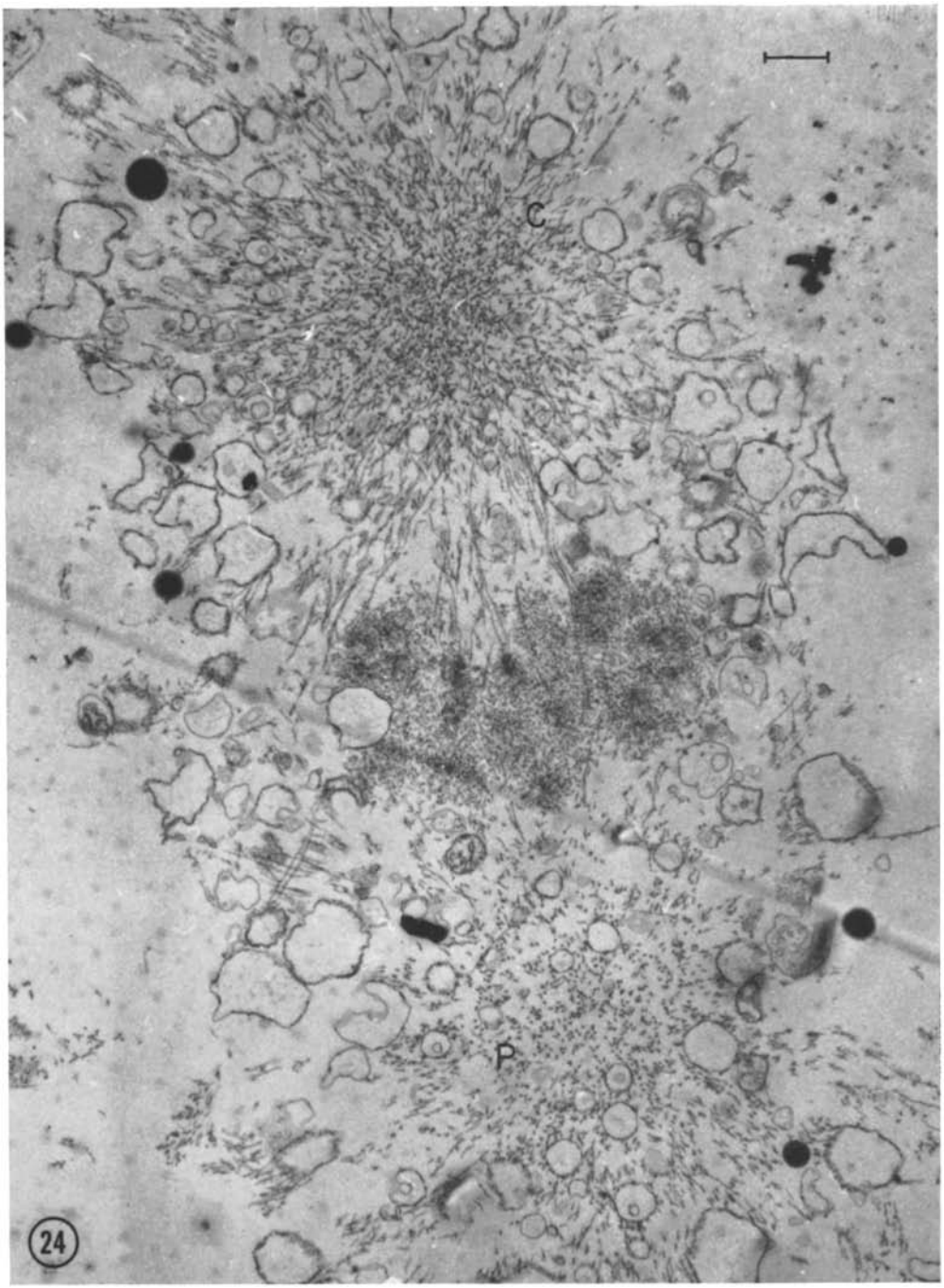

FIGURE 24 A hexylene-glycol–isolated MA from *S. solidissima* eggs. Arguments given in the text suggest that this MA is at a stage similar to the MA in Fig. 12. The line A—A in that figure gives the probable section through the MA seen in this micrograph. Chromosomes may be seen in the equatorial region. Fixation is with osmium textroxide as it is for all electron micrographs of MA presented except that in Fig. 36. × 8,000.

fixed with osmium tetroxide. It is unusual in that neither asters nor chromosomes have fallen off (see first section of Observations). By far, the major oriented components visible in this MA are the microtubules. One aster (*C*) appears larger than the other and contains a distribution of microtubule profiles varying from approximately circular (in the center) to quite long (in the periphery). The other aster (*P*) is more oval in over-all outline and possesses microtubule cross-sections with a considerably lower proportion of long profiles, especially where the spindle body and aster meet. The diffuse granular material at the MA equator is the chromosomal material; the denser parts probably are kinetochore attachments to the microtubules. This MA is interpreted as one whose migration to the egg surface has already occurred and results in a large central aster (C) and a flatter peripheral one (P) (see also Fig. 78 in reference 28, Mazia). The line A-A in Fig. 12 indicates the probable plane through the MA represented by Fig. 24, although no chromosomes are seen in Fig. 12.

The microtubules are about 240 A in diameter and have a wall thickness of about 70 A. In high-magnification electron micrographs the walls show indications of subunits (Fig. 25) although the subunits are by no means completely clear. In some micrographs, wisps of thin, filamentous material can be seen to continue from longitudinal profiles of microtubules (Fig. 29). Small particles associated with the microtubules are probably adherent ribosomes; they are present in small numbers. Vesicles, present throughout the MA, are either smooth surfaced or possess small granules on their surfaces. Occasionally a vesicle contains profiles reminiscent of cristae in mitochondria (Fig. 26); this suggests that the vesicle is a swollen mitochondrion. The profiles of these presumptive cristae appear to have attached small particles about 80–100 A in diameter. A small number of dense bodies with circular profiles are seen which are probably yolk granules (Fig. 24). None of these elements are found in the center of the aster although microtubules penetrate to the centriole. The region of exclusion of vesicles or granules is about 3.5 μ in diameter, surrounds the centriole, and probably constitutes the centrosomal region (59) (Figs. 27, 28).

Similar elements are seen in longitudinal sections through the axial regions of hexylene-glycol–isolated MA (Fig. 29). Fig. 30, at higher power,

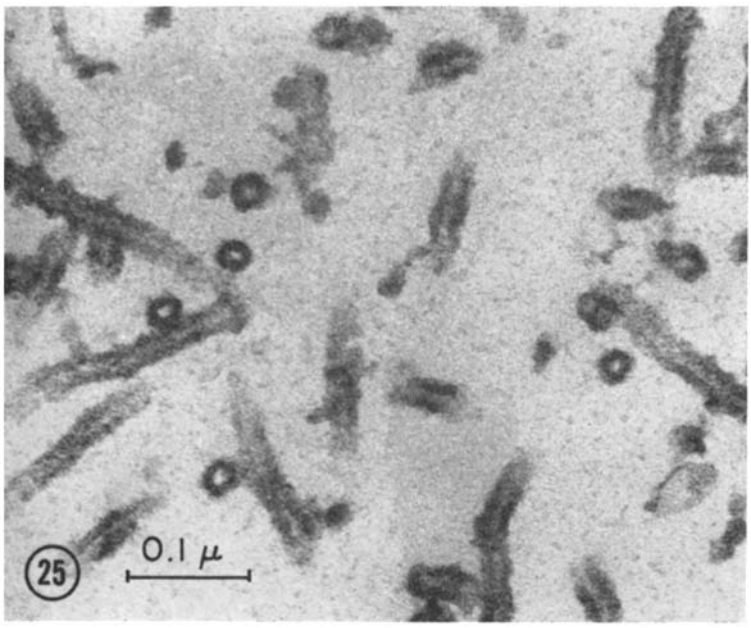

FIGURE 25 Higher magnification view of an MA of *S. solidissima* isolated as that in Fig. 24. Relatively few ribosome-like granules or membranous structures are present. × 160,000.

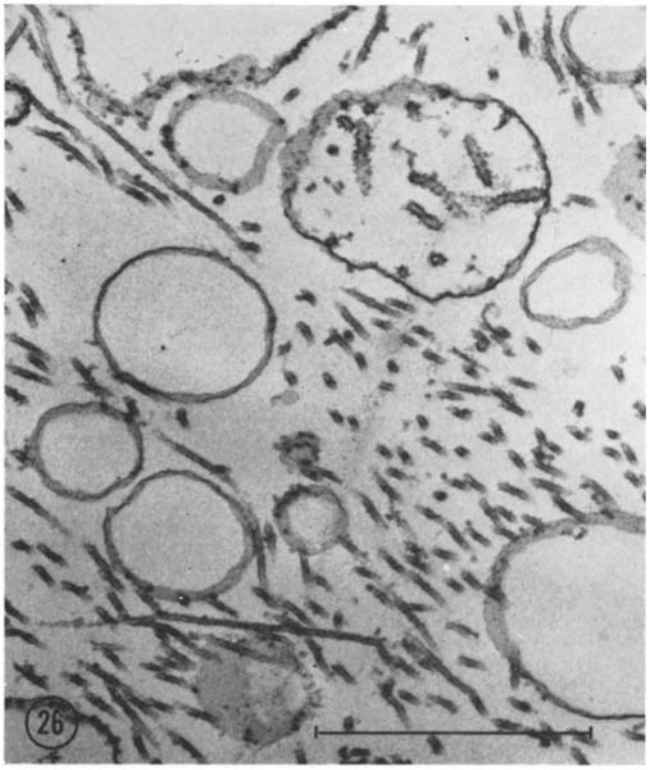

FIGURE 26 Peripheral portion of an aster from the 1st polar body MA of *S. solidissima* isolated with hexylene glycol. Some vesicles have smooth walls, some have small granules, and some appear to be swollen mitochondria with remnants of cristae in them. The latter appear to have granules about 100 A in diameter associated with them × 37,000.

indicates the cleanliness of these preparations with respect to the low concentration of material other than microtubules (and vesicles).

It should be noted that the microtubules in many of these preparations are not straight but are somewhat irregularly kinked. In addition, while most microtubules are roughly parallel to the spindle axis, some occasionally cross the rest at angles of up to 30° to the spindle axis (Fig. 29).

The same elements are visible in the MA prepared by rapid freezing (Fig. 31). With this technique the microtubules are 230 A in diameter, their walls being thinner (about 40 A thick) and more delicate than with chemical fixation. The microtubules themselves appear straighter with few kinks, and fewer or no wisps of material are seen continuing from microtubular profiles.

Figs. 32 and 33 are electron micrographs of hexylene-glycol–isolated *S. purpuratus* MA. They have essentially the same elements as *S. solidissima* MA. However, the vesicles, ribosomes and other background material are considerably greater in amount in the sea urchin than in the clam MA and may form the bulk of material in sea urchin MA. Frozen-substituted MA (Fig. 34) show components similar to those seen in fixed MA and, although the number of vesicles appears less than in the fixed MA, this is extremely variable from preparation to preparation and from region to region in the MA. A feature seen in *S. purpuratus* MA but not observed in *S. solidissima* MA is the frequent lateral association of two or more microtubules (Fig. 34). Although difficult to see clearly, an impression is gained of the existence of some substance between microtubules, perhaps acting as a bonding agent.

Figs. 27, 28, and 35 are electron micrographs of ethanol–isolated *S. solidissima* MA. The vesicular material and adherent material on the microtubules in these MA are greater in amount than on the microtubules in the MA (of this species) isolated in hexylene glycol although this is best seen after comparison of a number of electron micrographs of MA isolated with the two agents. In general, for both the clam and sea urchin, hexylene-glycol–isolated MA appear emptier than

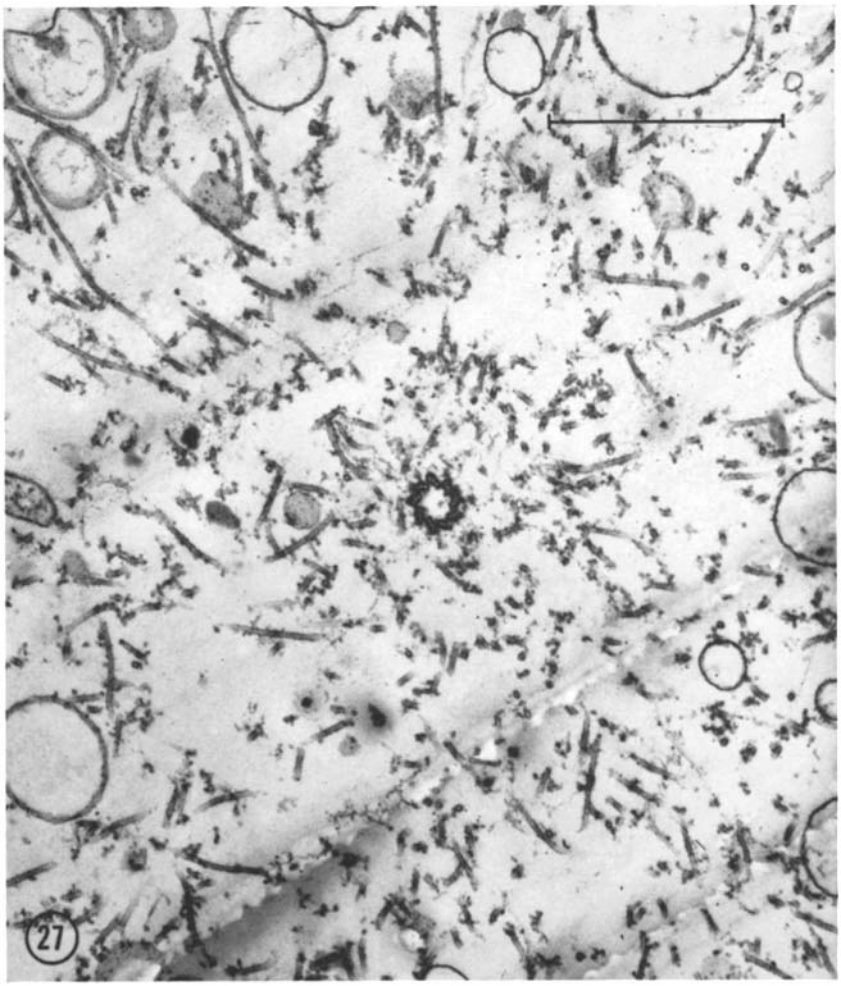

FIGURE 27 Cross-section through the centriole in an ethanol-isolated first polar body MA from *S. solidissima*. Microtubules penetrate to the centriole but vesicles are excluded from a region about 3.5 μ in diameter centered on the centriole. Ethanol-isolated MAs generally have nondescript, ragged wisps of material associated with microtubules which is not seen in hexylene-glycol–isolated MA. × 30,000.

ethanol-isolated ones. It is presumed that the "extra" material seen after ethanol isolation is derived from material which is evident in the MA region in intact eggs and which is less efficiently removed by ethanol during isolation.

Fig. 36 is an aster which was isolated from *S. solidissima* by the hexylene-glycol method, fixed with glutaraldehyde and postfixed with osmium tetroxide. No differences in components or their structure are seen in asters or MA fixed in this way compared to asters or MA fixed with osmium tetroxide alone.

DISCUSSION

Birefringence is an extremely important property of the MA, the values and fluctuations of which have figured prominently in theories of MA function (7, 15, 51, 56) and structure (7, 15). However, an interpretation of the meaning of birefringence on the molecular level, in terms of molecular rearrangements and changes which may be of importance in mitotic mechanisms, has been most elusive. Indeed, the structures responsible for birefringence in the MA have not yet been identified

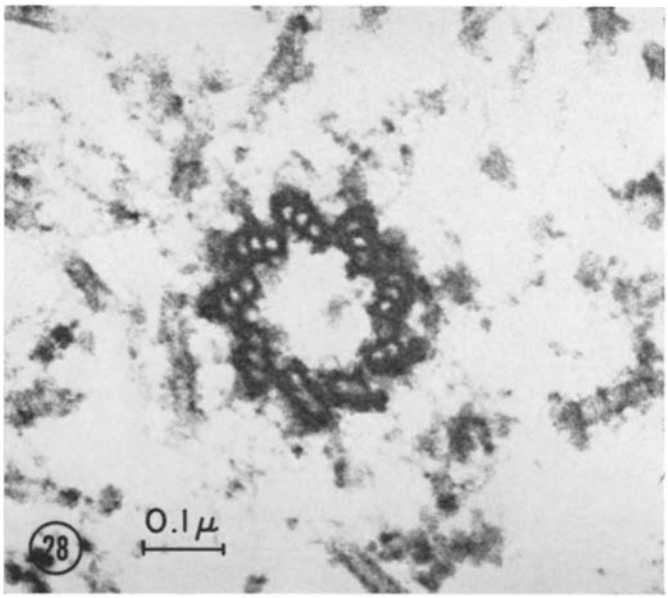

FIGURE 28 High-power electron micrograph of the centriole in the previous figure. × 104,000.

with certainty though the evidence points strongly toward the microtubules as major factors, as we shall now discuss. First, these structures are the most prominent oriented elements seen in the electron micrographs of MA so far produced. This is true for MA in intact cells (9–11, 41–43) as well as for isolated MA (21). Second, loss of birefringence of MA with time is accompanied by a breakup or loss of microtubules, both events occurring in parallel (8, 25). Third, the increase in birefringence of MA of marine eggs in the presence of D_2O (18) is accompanied by a corresponding increase in number of microtubules (17, 19); a similar relation appears to hold for MA whose birefringence has been increased by other agents (reference 38, Rebhun and Sander and unpublished data). Further, in other systems, such as the axopods of Heliozoa, a loss of the birefringent axial-rod (58) after cold- or colchicine treatment is accompanied by a loss of the microtubules of which the axial rod is composed (57). These data provide arguments for supporting the identity of the birefringent elements of intact cells with the microtubules. However, the evidence does not directly *establish* microtubules as the structures giving rise to birefringence, as likely as this seems, and certainly does not establish them as the sole elements contributing birefringence to the in vivo MA. For example, with respect to the latter point, Forer (7) has presented data which indicate that at least two oriented factors exist in the MA, one of which is possibly supportive in function and the other possibly involved in developing the motive force for chromosome movement. As yet, no second, oriented element has been positively identified in MA with the electron microscope. In another direction, experiments in this laboratory have indicated that the degree of aggregation or dispersion of the ribosomal material on the microtubules influences the retardation as measured in isolated sea urchin MA. Further, the disappearance of microtubules from isolated MA does *not* necessarily eliminate all birefringence from MA (8). Finally, in a recent paper, Behnke and Forer (4) argue that in crane-fly spermatocytes the microtubules cannot give rise to birefringence because the distribution of microtubules seen in the electron microscope and that of birefringent material are not the same. Indeed, they claim to find many microtubules in interzonal regions where they find no birefringence.

Some doubt may, therefore, attend acceptance of the identification of microtubules with all (or even any) of the birefringent material in in vivo or isolated MA.

Thus, we are faced with two questions: first, do the microtubules give rise to birefringence at all; and second, if so, is the birefringence of the in vivo MA solely due to microtubules. The easier question to answer is the first. The data on isolated

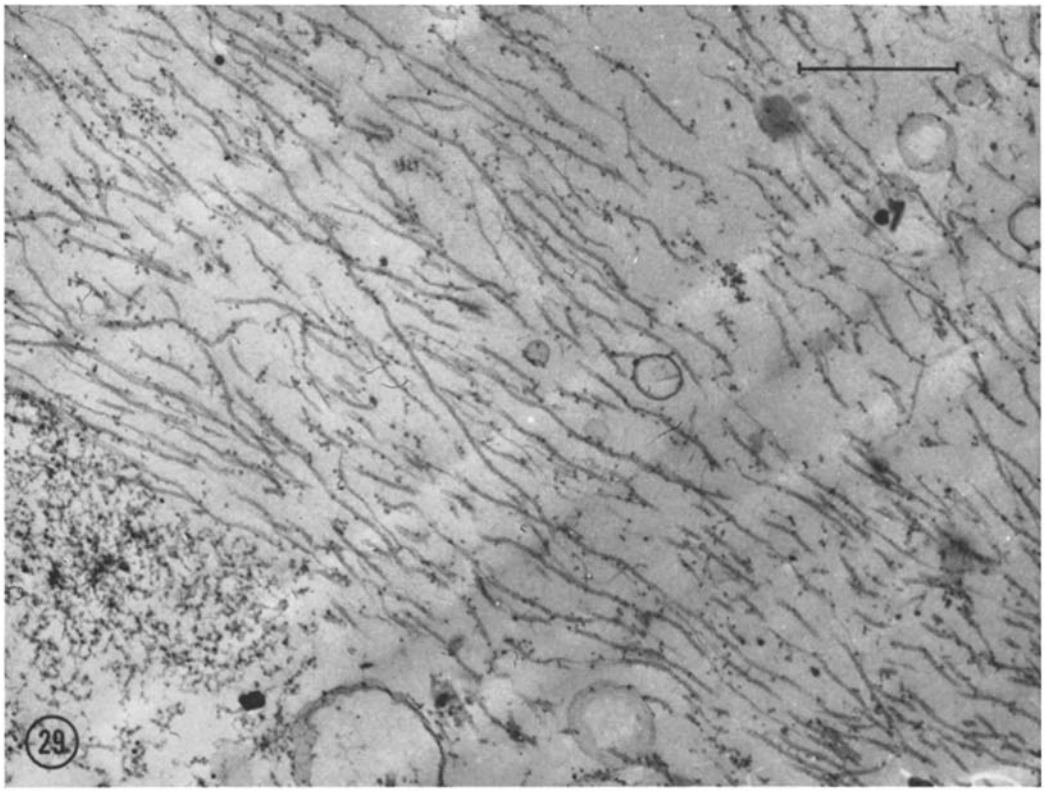

FIGURE 29 Longitudinal section of a hexylene-glycol-isolated first polar body MA of *S. solidissima*. Components similar to those in previous figures may be noted. Note also the local irregularities in the microtubules and wisps of filamentous material continuing from some of their profiles. × 21,000.

MA of *S. solidissima* appear to provide a relatively unequivocal "yes" answer, as will now be discussed.

S. solidissima MA do not appear to contain any significant background material between the microtubules other than swollen vesicles. A possible second, oriented component associated with the microtubule is the thin, wispy material occasionally seen continuing from the ends of the microtubules (Fig. 29). However, this most likely originates from sectioning of microtubules so that only part of the wall is included in the section. The presence of this wispy filamentous material in greater abundance in fixed MA as opposed to frozen MA is probably due to some breakdown and greater irregularity of the fixed microtubules. We have looked extensively for the presence of a microfilamentous structure applied to the MA microtubule surface but have not as yet seen evidence of it in these preparations, although such evidence would support speculations we have made (36) as to the possible force-generating element in mitotic movements.

It might be argued that there *is* material between microtubules, but that such material is not observable in the electron microscope with our techniques. Although the present data make it difficult to eliminate this argument, we offer the following observations for consideration in support.

First, we have used two preparative techniques for studying the MA in the electron microscope: chemical fixation and freeze-substitution. With both techniques the results are essentially the same in terms of components present and over-all morphology seen, the major difference being the greater thickness of the microtubule wall in fixed preparations relative to frozen ones. Second, the isolated MA of *S. solidissima* look remarkably "delicate" compared to those of *S. purpuratus* when observed with either the phase (20) or

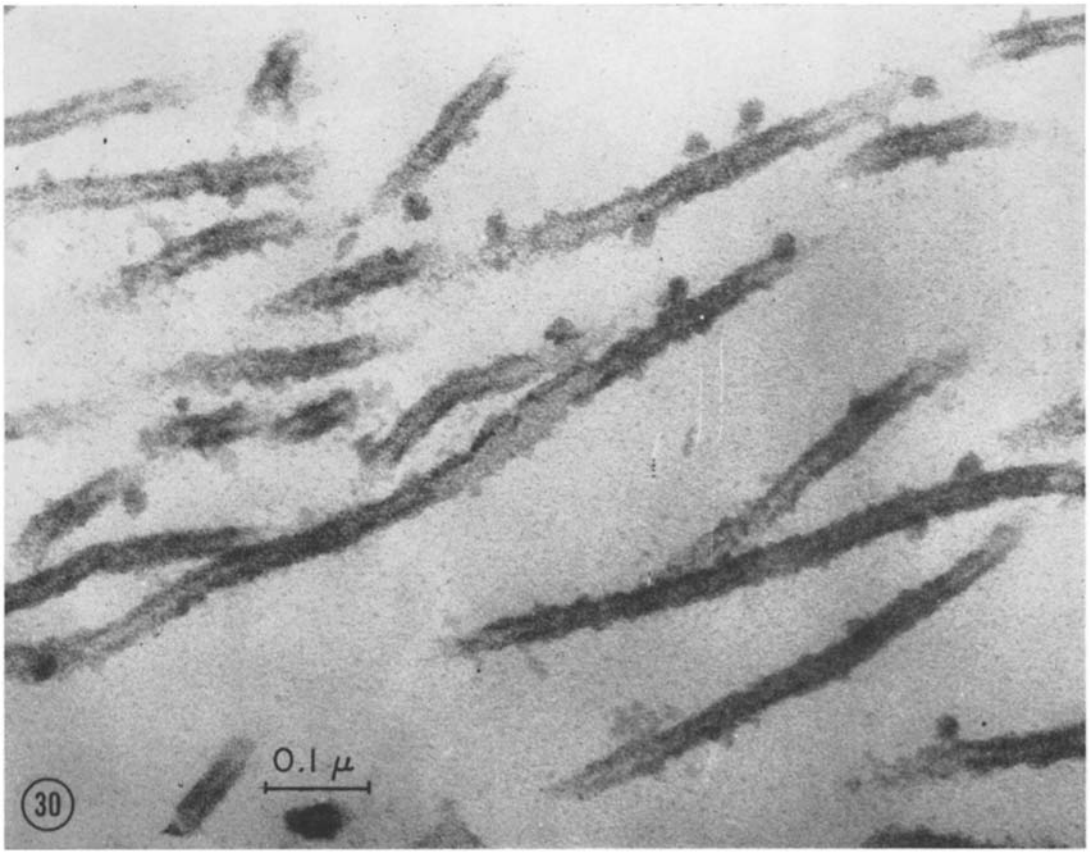

FIGURE 30 A longitudinal section of an MA similar to that in Fig. 29 showing cleanliness of the MA with respect to nonmicrotubular material. Compare to Fig. 25. × 130,000.

polarization microscope. Thus, one can easily "see through" the *S. solidissima* MA, in either the spindle or astral regions. In *S. purpuratus* MA, it is very clear that the birefringent elements are embedded in background material of considerable density. This can be seen with the polarizing microscope, e.g., compare Figs. 1 and 8. For the phase microscope image, one may compare any of the figures in Rebhun and Sharpless (37) for *S. solidissima* with those in Kane (20) for *S. purpuratus*. It is the transparency of the isolated *S. solidissima* MA, when examined by phase, polarization and electron microscope techniques, which convinces us that any material between the microtubules, other than vesicles, if it exists, must be present in very low quantity.

Thus, the correlation of the birefringence of the *isolated* MA of *S. solidissima* with the presence of oriented microtubules is direct. There is no evidence for *any* other oriented component which *can* give rise to birefringence in this material. It should be emphasized that this result is for *isolated* MA and does not necessarily hold for in situ MA.

With respect to the refractive index measurements in *S. solidissima*, the evidence suggests that most of the n is also due to the microtubules. The only competing elements are the small number of ribosome-like particles and the entrapped membranes. Since the ribosome-like particles are present in very small numbers, we would not expect them to contribute more than 4–5% of the total mass and therefore n of the MA, if that. The membranes constitute considerably greater bulk. However, the n measurements were made near the equatorial regions and in the ends of the large astral rays where fibers are free from vesicles. Although observations are difficult to make near the match point, it is generally the case that fibers are visible

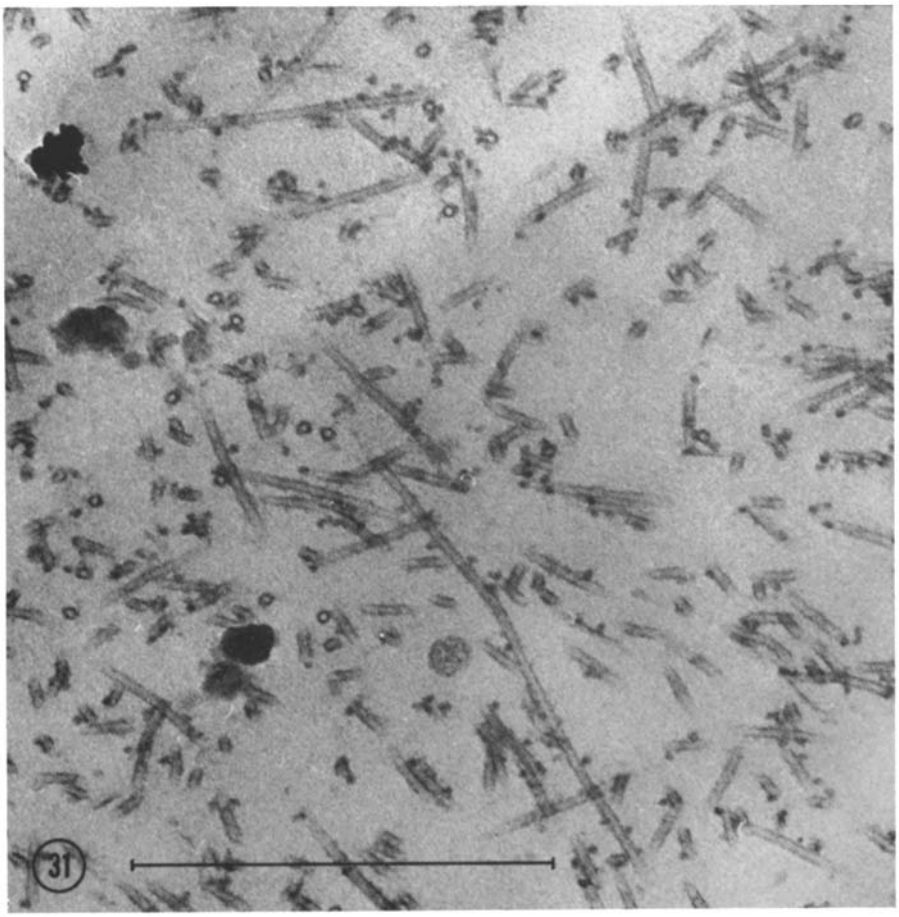

FIGURE 31 Section through the aster of a first polar body MA of *S. solidissima* prepared by freeze-substitution (see text). Note the absence of material other than components already described in preceding figures and, especially, the low concentration of nonmicrotubular material. × 56,000.

on either side of this n but not at it, except for a slight, tan coloration of the fibers due to osmium-tetroxide fixation. Thus, to a good approximation, the n measurements give us values for the fibers. Again, correlating the refractive index data with morphology in *S. solidissima* MA as seen in the electron microscope, we may say that the n values are those of the fixed microtubules since little else is present in the fibers which can contribute mass and, thus, refractive index.

Therefore, the electron microscope studies allow both birefringence and n to be related directly to microtubules in isolated *S. solidissima* MA. This allows us to say with some confidence that the residual, positive birefringence seen at the n match point is, indeed, the intrinsic birefringence of the microtubules, that is, the birefringence present when the n of the medium equals the average n of the MA (44). This result qualitatively agrees with the positive intrinsic birefringence measured for a variety of α-helical and non α-helical protein fiber systems, e.g. f-actin, paramyosin, and tobacco mosaic virus, by Cassim and Taylor (5).

These statements clearly cannot be made for isolated sea urchin MA. The ribosome-like particles in the background are extensively deployed throughout the intermicrotubular region and must constitute a considerable part of the MA mass. The n measurements clearly cannot be directly related to microtubules alone in this material. Further, as indicated above, work in our labora-

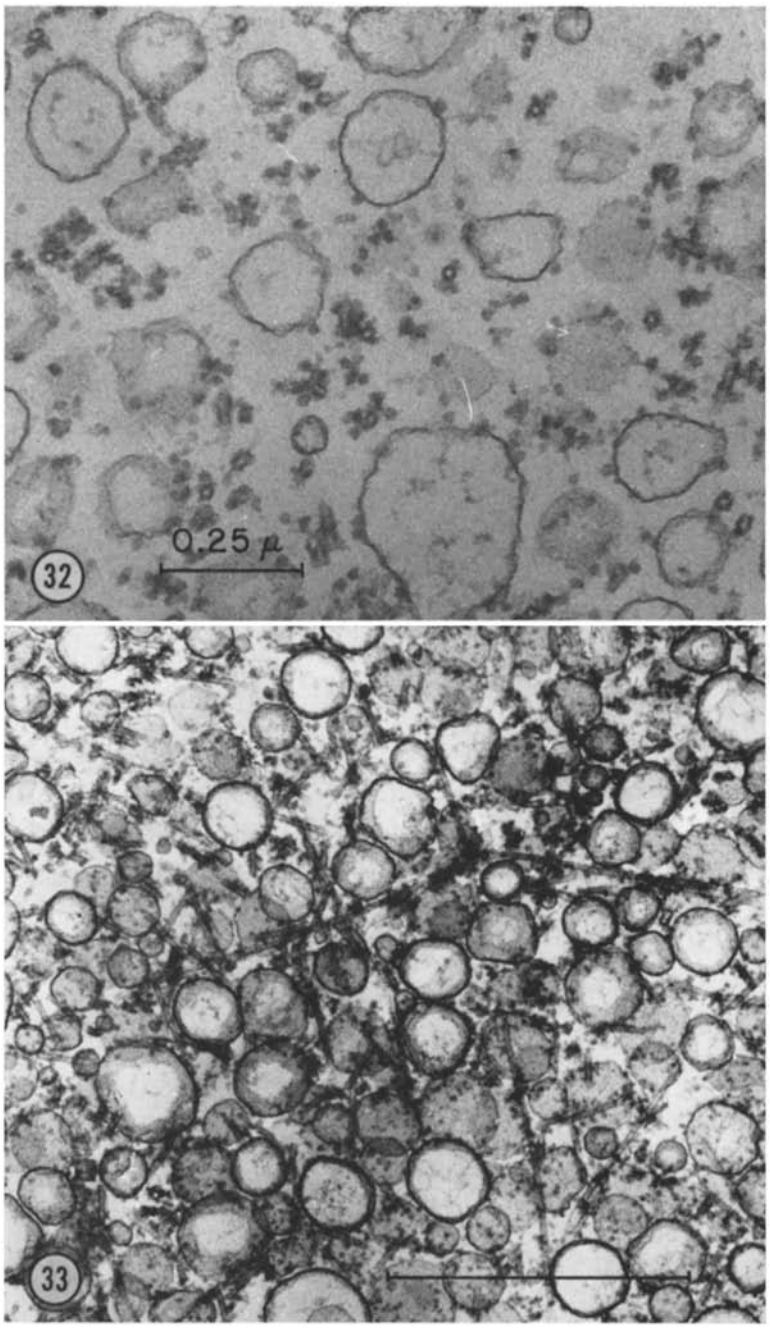

FIGURE 32 A cross-section through a hexylene-glycol–isolated MA from *S. purpuratus*. Note the large number of vesicles, presumably swollen elements of the endoplasmic or agranular reticulum. Note also the large number of ribosome-like granules either aggregated about microtubules or in isolated clusters between them. Similar elements may be seen in longitudinal sections of these MA. × 72,000.

FIGURE 33 Section through an aster of an MA of *S. purpuratus* isolated as that in Fig. 32 and showing similar elements. × 39,000.

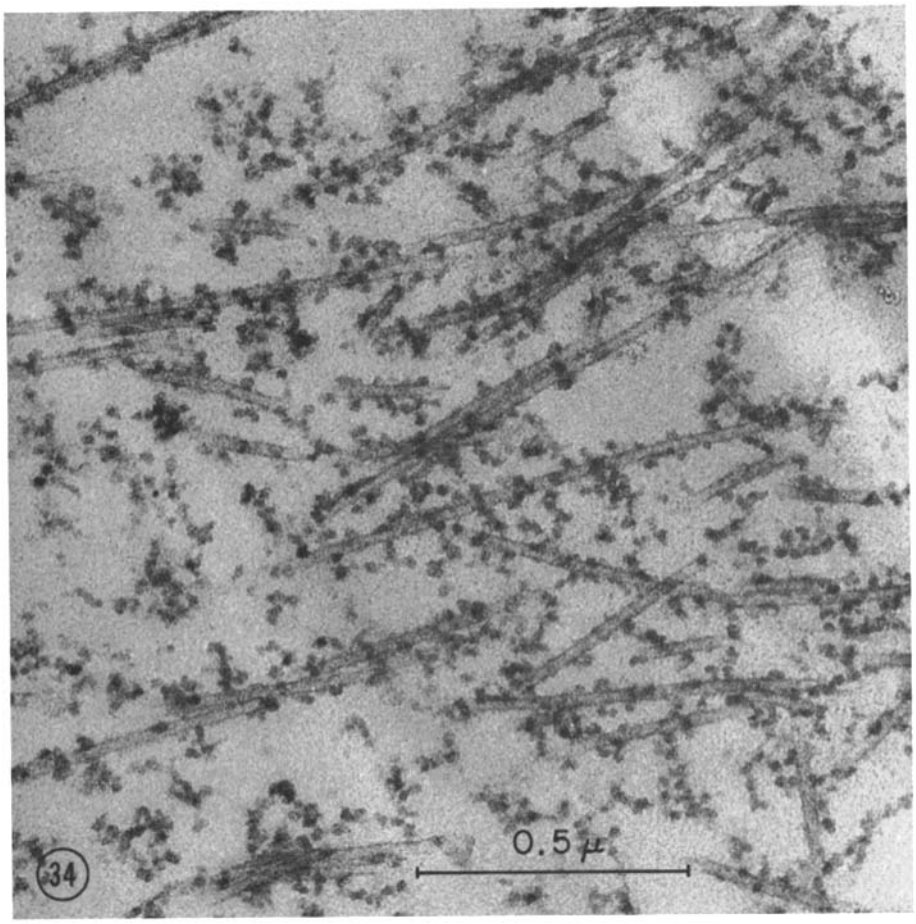

FIGURE 34 Longitudinal section of an MA from *S. purpuratus* isolated in hexylene glycol and prepared by freeze-substitution (see text). Microtubules and ribosome-like material are abundant. No vesicles are seen but the number present depends upon the part of the MA sectioned and the particular batch of MA observed. In general, MA prepared by either chemical fixation or freeze-substitution show similar components and structure. Note the lateral association of microtubules. × 72,000.

tory by Goldman (8) indicates that form birefringence may be contributed by aggregations of ribosome-like particles on the microtubules. Form birefringence for such linear aggregates is expected on theoretical grounds (5). Birefringence cannot, therefore, be directly related to microtubules alone in these MA.

Since, however, the results for clam MA discussed above show that microtubules are capable of giving rise to strong birefringence, since the values of retardation for clam and sea urchin MA are not greatly different, and since MA from sea urchin contain similar numbers of microtubules oriented like those in MA from *S. solidissima*, it is strongly suggested that microtubules contribute a significant and probably major amount of the birefringence of sea urchin MA. However, since data of Goldman (8) indicate that up to one-third of the measured retardation in isolated *S. purpuratus* MA may be contributed by the nonmicrotubular material, the interpretation of birefringence is clearly more complex in sea urchin MA than in clam MA. Thus, while the results for isolated *S. solidissima* MA clearly support the statement that oriented microtubules give rise to birefringence, those for isolated *S. purpuratus* MA just as clearly demonstrate the possibility that microtubule bire-

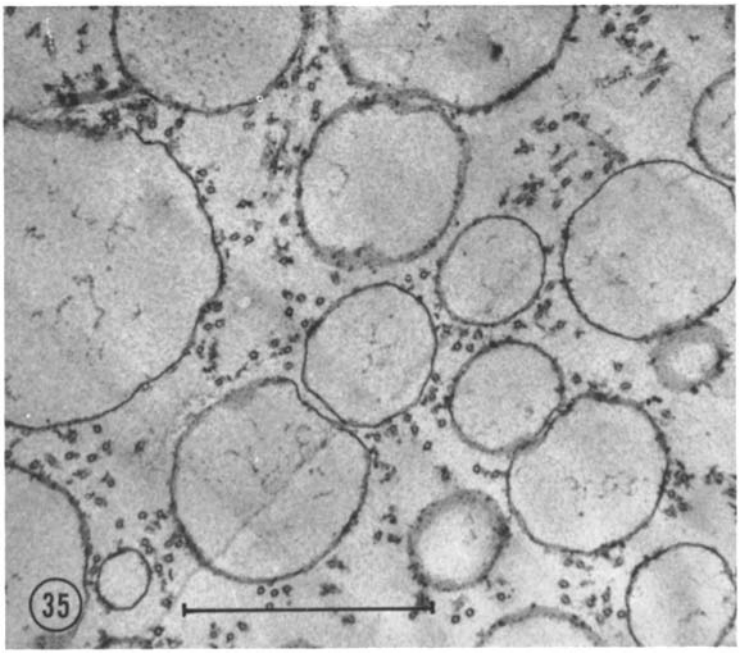

FIGURE 35 Cross-section of the spindle region of an MA isolated as that in Fig. 27, from the same organism and stage. Note the large number of vesicles in these ethanol-isolated MA compared to those in hexylene-glycol–isolated MA (Figs. 24 and 25) of the same organism. The microtubules, again, have some adherent material, less obvious in this lower power micrograph. × 33,000.

fringence may be modified by other material oriented by microtubules.

It is expected that in the in vivo MA the origin of birefringence may be even more complex than in the isolated sea urchin MA. Indeed, if other components are associated with microtubules in vivo, they may modify the measured retardation either by contributing negative or positive birefringence or merely by causing local changes in refractive index. Because of the preponderant form birefringence of the MA demonstrated in this paper and in that of Pfeiffer (31), such changes in refractive index will result in changes in observed retardation. Evidence for the presence of such substances has been presented, e.g. by Rustad (46), in MA of *S. purpuratus* isolated by an older method, where an increase in mass (measured interferometrically) and in RNA occurs in the interzonal region at midanaphase. Another source of modification of the microtubule birefringence may be oriented cisternae of the granular or agranular reticulum, which could contribute birefringent material whose sign is negative relative to the MA axis (44). This can be expected to occur since cisternal elements do orient in the MA (33, 42) with planar surfaces parallel to the microtubules. Further, it was pointed out by Inoué and Dan (16) that astral fibers could be negatively birefringent, probably owing to the compression they suffer during late anaphase when the MA has considerably elongated and is pressing astral fibers against the egg cortex. If the pole-to-pole fibers of the MA are under compression during anaphase, their retardation may, indeed, be reduced or possibly even reversed if the observations for astral fibers hold also for pole-to-pole fibers. Indeed, we have on occasion seen negatively birefringent pole-to-pole fibers (Observations). Finally, changes in spatial distribution of microtubules at different stages of cytokinesis could give rise to differences in observed retardation since birefringent rods uniformly distributed in a given volume will show considerable differences in local retardation compared to the same number nonuniformly aggregated in the same volume. It is clear, therefore, that the origin of birefringence and its dynamic changes in terms of the distribution of ultrastructural elements giving

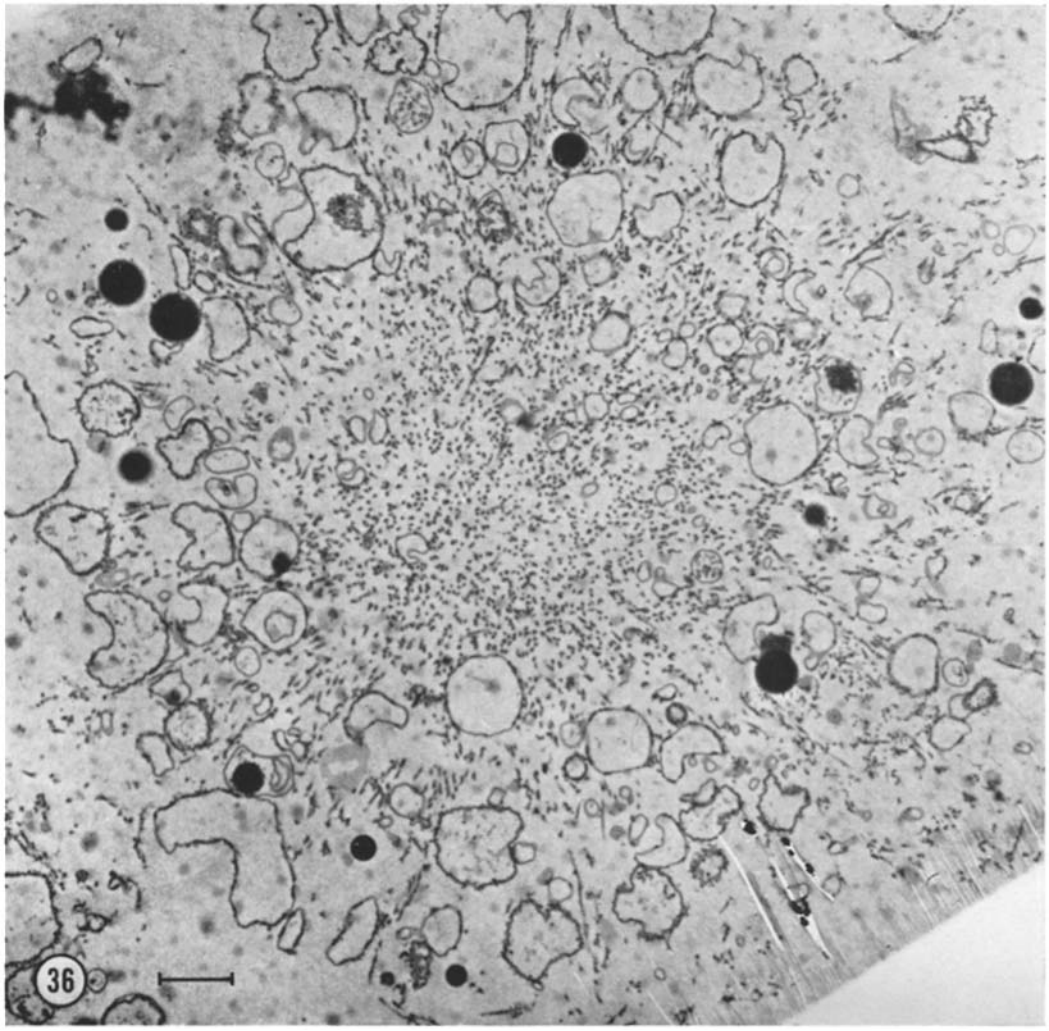

FIGURE 36 A section through an aster isolated with hexylene glycol from *S. solidissima*. Fixation is with glutaraldehyde, in contrast to the fixation used for all other electron micrographs in this paper. The elements seen are the same as those seen after OsO_4 fixation, no differences appearing in any particulars. × 10,000.

rise to it in the living MA is bound to be complex. It is with these considerations in mind that one should evaluate the statement in Behnke and Forer (4) that microtubules cannot give rise to birefringence in the MA because microtubules, but not birefringence, are found in the interzonal regions during anaphase in crane-fly spermatocytes.

Thus, we have arrived at the following conclusions. (*a*) The birefringence of isolated MA of both clam and sea urchin eggs is primarily positive form birefringence with a residual positive intrinsic birefringence. (*b*) The isolated MA of *S. solidissima* eggs are composed primarily of microtubules, assorted vesicles, and very few ribosome-like particles. (*c*) Isolated MA of sea urchin eggs contain many more ribosomal-like particles and vesicles than do isolated MA of clam eggs. These particles and vesicles form a large portion, if not the bulk, of the MA material. (*d*) Essentially the same components are seen in frozen-substituted MA as in chemically fixed, isolated MA. However, in the

former preparations the microtubules are straighter and possess thinner walls. (*e*) Microtubules of MA isolated with ethanol have more material adherent to them: they appear "dirtier." (*f*) Electron microscope, polarization microscope, and phase microscope observations on isolated *S. solidissima* MA indicate that there is little, if any, diffuse material between the microtubules. Since no other oriented material exists, this allows the inference to be drawn that in these MA it is the microtubules alone which give rise to birefringence and to most of the refractive index. (*g*) Neither of the conclusions in (*f*) holds for isolated sea urchin MA since much aggregated ribosomal material adheres to the microtubules. This material contributes to the refractive index and most likely to some of birefringence of the MA. However, the major part of the birefringence of sea urchin MA also appears to be due to microtubules. (*h*) In the in vivo MA the situation is likely to be even more complex since modifying or masking substances may alter birefringence as may compression or tension exerted on the MA.

The abundance of microtubules relative to other components in the isolated clam MA compared to sea urchin MA may offer a considerable advantage in the interpretation of the origin of material seen in dissolved MA with optical ultracentrifugation and other techniques (24, 47, 54). Investigation in this direction is now underway.

This work has been supported by Research Grants from the National Science Foundation and the National Institutes of Health.

We wish to thank Dr. R. D. Allen for his advice and the use of some of his equipment in the early stages of this work.

Received for publication 27 January 1967.

BIBLIOGRAPHY

1. Allen, R. D., and H. Nakajima. 1964. *Exptl. Cell Res.* **37**:230.
2. Bajer, A., and R. D. Allen. 1966. *Science.* **151**: 572.
3. Barer, R. 1956. Chapter 2. *In* Physical Techniques in Biological Research. G. Oster and A. Pollister, editors. Academic Press Inc., New York. **3**.
4. Behnke, O. and A. Forer. 1966. *Compt. Rend. Lab. Carlsberg.* **35**:437.
5. Cassim, J. Y. and E. W. Taylor. 1965. *Biophys. J.* **5**:531.
6. Dan, K., S. Ito, and D. Mazia. 1952. *Biol. Bull.* **103**:292.
7. Forer, A. 1966. *Chromosoma.* **19**:44.
8. Goldman, R. D. 1967. The structure and some properties of the isolated MA. Ph.D. Thesis. Princeton University, Princeton, New Jersey.
9. Harris, P. 1962. *J. Cell Biol.* **14**:475.
10. Harris, P. 1965. *J. Cell Biol.* **25**:(1 Pt. 2): 73.
11. Harris, P., and A. Bajer. 1965. *Chromosoma.* **16**:624.
12. Hughes, A. 1952. The Mitotic Cycle. Butterworth & Co. (Publishers) Ltd., London.
13. Inoué, S. 1952. *Exptl. Cell Res. Suppl.* **2**:305.
14. Inoué, S. 1952. *Biol. Bull.* **103**:316.
15. Inoué, S. 1964. *In* Primitive Motile Systems in Cell Biology. R. D. Allen and N. Kamiya, editors. Academic Press, Inc., New York, 549.
16. Inoué, S., and K. Dan. 1951. *J. Morphol.* **89**:423.
17. Inoué, S., and H. Sato. 1967. *J. Gen. Physiol.* **50** (6, Pt. 2):259.
18. Inoué, S., H. Sato, and R. W. Tucker. *Biol. Bull.* **125**:380.
19. Inoué, S., H. Sato, R. Kane, and R. Stephens. 1965. *J. Cell Biol.* **27**:115A.
20. Kane, R. E. 1962. *J. Cell Biol.* **12**:47.
21. Kane, R. E. 1962. *J. Cell Biol.* **15**:279.
22. Kane, R. E. 1963. *Biol. Bull.* **125**:381.
23. Kane, R. E. 1965. *J. Cell Biol.* **25**:137.
24. Kane, R. E. 1967. *J. Cell Biol.* **32**:243.
25. Kane, R. E., and A. Forer. 1965. *J. Cell Biol.* **25**:31.
26. Köhler, A. 1921. *Z. Wiss. Mikroskopie.* **38**:29.
27. Luft, J. H. 1961. *J. Biophys. Biochem. Cytol.* **9**:409.
28. Mazia, D. 1961. Chapter 2. *In* The Cell. J. Brachet and A. E. Mirsky, editors. Academic Press, Inc., New York. **3**.
29. Mazia, D., and K. Dan. 1952. *Proc. Natl. Acad. Sci. U. S.* **38**:826.
30. Mazia, O., J. M. Mitchison, H. Median, and P. Harris. 1961. *J. Biophys. Biochem. Cytol.* **10**:467.
31. Pfeiffer, H. H. 1952. *Pubbl. Staz. Zool. Napoli.* **23** (Suppl.):147.
32. Rebhun, L. I. 1959. *Biol. Bull.* **117**:518.
33. Rebhun, L. I. 1960. *Ann. N. Y. Acad. Sci.* **90**:857.
34. Rebhun, L. I. 1965. *Federation Proc.* **24** (Suppl.): S217.
35. Rebhun, L. I. 1966. *In* Freeze-Drying. L. Rey, editor. Hermann et Cie, Paris, 133.
36. Rebhun, L. I. 1967. *J. Gen. Physiol.* **50** (6 Pt. 2): 223–239.
37. Rebhun, L. I., and T. K. Sharpless. 1964. *J. Cell Biol.* **22**:488.

38. REBHUN, L. I., and G. SANDER. 1966. *Biophys. J.* **6**:46A.
39. REYNOLDS, E. S. 1963. *J. Cell Biol.* **17**:208.
40. ROSS, K. R. 1958. *In* General Cytochemical Methods. J. F. Danielli, editor. Academic Press Inc., New York. **2**:1.
41. ROTH, L. E. 1964. *In* Primitive Motile Systems in Cell Biology. R. D. Allen and N. Kamiya, editors. Academic Press Inc., New York. 527.
42. ROTH, L. E., H. J. WILSON, and J. CHAKRABORTY. 1966. *J. Ultrastruct. Res.* **14**:460.
43. ROBBINS, E., and N. K. GONATAS. 1964. *J. Cell Biol.* **21**:429.
44. RUCH, F. 1956. Chapter 4. *In* Physical Techniques in Biological Research, G. Oster and A. W. Pollister, editors. Academic Press Inc., New York. **3**.
45. RÜNNSTROM, J. 1928. *Protoplasma.* **5**:201.
46. RUSTAD, R. 1959. *Exptl. Cell Res.* **16**:575.
47. SAKAI, H. 1966. *Biochem. Biophys. Acta.* **112**:132.
48. SCHMIDT, W. J. 1928. *Naturwissenshaften.* **16**:900.
49. SCHMIDT, W. J. 1936. *Biodynamica.* **1**:1.
50. SCHMIDT, W. J. 1937. Die Doppelbrechung von Karyoplasma, Zytoplasma und Metaplasma. Gebrüder Borntraeger, Berlin.
51. SCHMIDT, W. J. 1939. *Chromosoma.* **1**:253.
52. SCHRADER, F. 1953. Mitosis. Columbia University Press, New York.
53. STEMPAK, J. C., and R. T. WARD. 1964. *J. Cell Biol.* **22**:697.
54. STEPHENS, R. 1967. *J. Cell Biol.* **32**:255.
55. SWANN, M. M. 1951. *J. Exptl. Biol.* **28**:417.
56. SWANN, M. M. 1951. *J. Exptl. Biol.* **28**:434.
57. TILNEY, L. G. 1965. *J. Cell Biol.* **27**:107A.
58. TILNEY, L. G., and K. R. PORTER. 1965. *Protoplasma.* **60**:317.
59. WENT, H. 1966. Protoplasmatalogia. Springer-Verlag, Wien. **6**:1.